

PAPER • OPEN ACCESS

Electron-neutral collision cross sections for H₂O: I. Complete and consistent set

To cite this article: Maik Budde *et al* 2022 *J. Phys. D: Appl. Phys.* **55** 445205

View the [article online](#) for updates and enhancements.

You may also like

- [MULTI-DIMENSIONAL FEATURES OF NEUTRINO TRANSFER IN CORE-COLLAPSE SUPERNOVAE](#)
K. Sumiyoshi, T. Takiwaki, H. Matsufuru et al.
- [Comparisons of sets of electron–neutral scattering cross sections and swarm parameters in noble gases: I. Argon](#)
L C Pitchford, L L Alves, K Bartschat et al.
- [Three-dimensional Boltzmann-hydro Code for Core-collapse in Massive Stars. III. A New Method for Momentum Feedback from Neutrino to Matter](#)
Hiroki Nagakura, Kohsuke Sumiyoshi and Shoichi Yamada








IOP | ebooks™

Bringing together innovative digital publishing with leading authors from the global scientific community.

Start exploring the collection—download the first chapter of every title for free.

Electron-neutral collision cross sections for H₂O: I. Complete and consistent set

Maik Budde^{1,2,*} , Tiago Cunha Dias² , Luca Vialetto³ , Nuno Pinhão² , Vasco Guerra²  and Tiago Silva² 

¹ Department of Applied Physics, Eindhoven University of Technology, 5600 MB Eindhoven, The Netherlands

² Instituto de Plasmas e Fusão Nuclear, Instituto Superior Técnico, Universidade de Lisboa, Av. Rovisco Pais, 1049-001 Lisbon, Portugal

³ Theoretical Electrical Engineering, Faculty of Engineering, Kiel University, Kaiserstraße 2, 24143 Kiel, Germany

E-mail: m.budde@tue.nl

Received 3 June 2022, revised 22 August 2022

Accepted for publication 30 August 2022

Published 12 September 2022



Abstract

This work proposes a complete and consistent set of cross sections (CSs) for electron collisions with water molecules to be published in the IST-Lisbon database on LXCat. The set is validated from the comparison between experimental and computed electron swarm parameters. The former are collected from literature while the latter are calculated using a space-homogeneous two-term Boltzmann solver, assuming isotropic scattering in inelastic collisions. Rotational CSs, based on the Born approximation, are optimised by means of the electron swarm analysis technique. Superelastic rotational and vibrational collisions are accounted for in the calculations and found to be particularly important for low-energy electrons interacting with water molecules. The set can be used with codes assuming space-homogeneous conditions, in particular common two-term Boltzmann solvers, ensuring a good agreement with experiments. Therefore, it constitutes an important tool for fast calculations and modelling of complex plasma chemistries.

Supplementary material for this article is available [online](#)

Keywords: H₂O, electron-neutral collision cross section, electron swarm technique, two-term Boltzmann solver, molecular rotation

(Some figures may appear in colour only in the online journal)

1. Introduction

An accurate characterisation of the interaction of water molecules and electrons is required in various fields of ongoing fundamental and application-oriented research. For instance,

* Author to whom any correspondence should be addressed.



Original Content from this work may be used under the terms of the [Creative Commons Attribution 4.0 licence](#). Any further distribution of this work must maintain attribution to the author(s) and the title of the work, journal citation and DOI.

their interaction is relevant in plasma-in-liquid [1], waste (-water) and wound treatment with plasma [2, 3], or because water is an omnipresent impurity in atmospheric plasma [4], spark-ignited combustion [5], plasma sterilisation [6] and CO₂ plasma conversion [7]. In these environments, electrons constitute the primary energy source to the heavy particles. Therefore, an accurate description of the electrons facilitates the understanding, tailoring and optimisation of water-containing discharges.

Electron-neutral collision cross sections (CSs), as provided here, are key to that description as they allow the calculation of the electron energy distribution function (EEDF)

from the electron Boltzmann equation. A wide-spread solution approach is the use of two-term, space-homogeneous Boltzmann solvers such as LoKI-B [8] or BOLSIG+ [9].

Despite the clear demand, to this point there is no commonly agreed-on comprehensive CS set available for water neither on LXCat [10], i.e. one of the most extensive open-access CS websites, nor elsewhere, although many authors have proposed different sets either derived from experiments or *ab-initio* calculations [11–25]. A set's comprehensiveness is defined by two requirements, namely completeness and consistency. A complete set for H₂O includes CSs for elastic, rotational, vibrational, electronic excitation, dissociation, ionisation and electron attachment collisions. When striving for the CSs, some studies [11, 13, 16] present valuable compilations of CSs, e.g. the recent extensive review by Song *et al* [16] but neglect the second requirement to a CS set that is consistency. A CS set must be validated against measurements [15, 17, 18, 26]. The macroscopic parameters derived from the solution of the Boltzmann equation, using the CS set presented here, are hence validated against experimental electron swarm parameters. Eventually, a complete and consistent set is obtained that is immediately usable for everybody due to the optimisation by means of the openly accessible two-term Boltzmann solver LoKI-B v2.1.0 [8].

The optimisation of swarm calculations for H₂O is particularly challenging due to the variety and number of elementary processes involved, and attention must be paid to the assumptions taken prior to the optimisation of the CSs. For this reason, we decided to split the study into two contributions. In this work, we present a complete and consistent set of CSs that is derived under the assumptions of (i) two-term solutions of the electron Boltzmann equation, (ii) isotropic scattering in inelastic collisions, and (iii) equal energy sharing between scattered and secondary electrons in ionisation events. The assumptions come with well-known limitations like the restriction to small reduced electric fields, i.e. small anisotropy [27]. In a forthcoming second paper, we intend to evaluate these assumptions, e.g. through inclusion of anisotropy, and compare two-term Boltzmann solver calculations with multi-term and Monte Carlo simulations.

Probably the main reason for the ongoing discussion of H₂O CSs is molecular rotations. Even though there is consensus in the community about the importance of rotations, especially for collisions with low-energy electrons, they are often not included properly in the CS sets. For instance on LXCat [10], at the time of writing this manuscript, some databases do not include rotations [12, 28, 29] or only provide lumped CSs (three in [30] and one in [31] in total). Other studies offer detailed rotational CSs but either the CSs or the used software are not openly accessible [15, 17]. Although CS and program should be independent, verification is impeded in these situations.

Henceforth, the objective of our work is clear, namely to provide a complete and consistent CS set for electron collisions with water molecules considering the most recent CSs and swarm data, including rotational collisions, to be used in an openly available standard two-term solver. The anticipated open-access release in the IST-Lisbon database [32] on LXCat

gives the community the tools to include water in their plasma chemistry models.

2. Molecular quantum state of water

This section introduces to rotations of water molecules, required to treat rotational collisions with electrons. First, the rotational quantum state is characterised, second, peculiarities in the populations of rotational levels and transitions between them are discussed.

Inclusion of rotational collisions requires the proper characterisation of rotational states as presented in the following. The rotational state is denoted as J . The H₂O molecule is an asymmetric-top rotor, i.e. it has three different finite moments of inertia which makes the description of the rotational state more complex than for a linear molecule like CO [33, 34]. In consequence, in addition to the principal rotational quantum number J (not to be confused with the notation of the rotational state itself J), two more quantum numbers are required. These are K' and K'' , the projection of J along the axis of the smallest and largest moment of inertia, respectively. As of now, the rotational state is given by the three numbers $J = JK'K''$.

Next, we need to understand which rotational transitions to consider and how. Depending on the nuclear spin orientation of the two hydrogen atoms of the molecule, water is divided in two sets of spin isomers with different properties and nearly no interaction between the two. The pseudo-quantum number $\tau = K' - K'' = -J, -J + 1, \dots, J$ is introduced [33], allowing to distinguish ortho-water (parallel nuclear spins) with odd τ and para-water (antiparallel nuclear spins) with even τ . Rotational transitions are only allowed within a set. At the same time, the statistical weight of a rotational state and thereby its population depends on the type of isomer of water [35]. The statistical weight is

$$g_{\text{rot}}(J, \tau) = (2J + 1)g_s(\tau)g_i. \quad (1)$$

Here, J is again the principal rotational quantum number, g_s the state-dependent nuclear spin statistical weight as a function of τ which is 1 for para- and 3 for ortho-water, respectively, and g_i the state-independent nuclear spin statistical weight which is 1 for the most abundant water isotopologues [36]. A Matlab function to calculate $g_{\text{rot}}(J, \tau)$ to determine the level populations following a Boltzmann distribution at gas temperature, and the level energies required for that purpose are provided as supplementary material, see table 3 [37].

Finally, superelastic collisions are not only considered between rotational but also between vibrational states, indicated here as v . As a three-atomic molecule, water has three vibrational modes: (i) the symmetric stretching ν_1 , (ii) the bending ν_2 and (iii) the asymmetric stretching ν_3 . Thus, the vibrational state is characterised as $v = \nu_1\nu_2\nu_3$. Herein, a Boltzmann population distribution at gas temperature is assumed for the vibrational levels as well. The vibrational levels included in this set are indicated in table 1.

Table 1. Vibrational energy levels of water included in this work, vibrational energy with respect to the ground state and populations for a Boltzmann distribution at 293 K (given with the maximum accuracy accepted by BOLSIG+) [30].

$v_1v_2v_3$	Energy (eV)	Population
000	0.0	0.99961
010	0.198	0.00039
100 + 001	0.453	0.00000

3. The CS set

In this section, we present a throughout review of the CSs available in literature that are used as basis to construct our set. Furthermore, we present the final set of CSs that has been derived with the swarm analysis technique. In total, 163 CSs are considered.

Figure 1 shows the proposed CSs σ , plotted against the electron energy ε , divided into conservative collisions on the left with constant electron number and non-conservative processes, i.e. attachment and ionisation, on the right where the number of electrons changes. Among the available elastic CSs [12, 16, 30, 38] the one hard coded in the code Magboltz v11.9 by Biagi [38] gives the best immediate agreement with experimental swarm parameters. The solid black line in figure 1 represents this elastic CS after slight modification. As shown in figure 2, the high-energy tail of the elastic CS has been slightly decreased compared with the original CS, to better reproduce measurements of electron swarm parameters. Note the Ramsauer minimum at about 2.5 eV followed by a resonance [17] both customary well handled by LoKI-B [34].

The sum of the rotational CSs, each calculated according to Itikawa assuming the Born approximation [33] and weighted by the population of the initial rotational level at 293 K, is plotted as dashed line. It must be stressed that the sum is for illustration only, that is, in the actual calculation of the EEDF 147 individual rotational CSs are used. The Born approximation neglects short-range effects close to the threshold [19, 20]. Corrections due to the polar nature of the molecule, usually addressed by the Born-closure technique [13, 16, 20, 30], are not included neither beforehand nor implicitly by the code. Furthermore, we assume isotropic scattering which is why a forward angular discrimination correction [47] is not implemented. Arguments in favour of the Born approximation [48–50] and the obtained agreement with experiments in section 4 speak for the validity of the introduced simplifications. The lowest rotational level included is $\text{H}_2\text{O}(X, v = 000, J = 000)$ at 0 eV (reference value where X refers to the electronic ground state) while the highest level is $\text{H}_2\text{O}(X, v = 000, J = 660)$ at 0.12958 eV (given with the maximum accuracy accepted by BOLSIG+, like in table 1). This selection is in accord with the availability of line strength data from King *et al* [51] that is required for the calculation of the CSs. To better reproduce experimental measurements of electron swarm parameters, the rotational CSs derived from the Born approximation, are modified, under the assumption of isotropic electron scattering in the collisions. First, they are

all scaled down by a factor of 0.3. Similarly, Song *et al* multiplied rotational NO CSs by 0.3 [52] or Kawaguchi *et al* scaled down rotational CSs of H_2O by one order of magnitude [14]. The rotational CSs are then set to zero for electron energies larger than 12 eV, see figure 2 for illustration. Cutting the CSs at high energies leads to a better agreement with the reduced Townsend coefficient in figure 3. The importance of rotations is highlighted in figure 4 that shows the EEDFs of water with (dash-dotted lines) and without (solid lines) the 147 rotational CSs. Especially, at low reduced electric field of 10 Td a large difference between the two calculations is observed because at that E/N many electrons have low energy corresponding to large rotational CSs, despite the low energy losses in rotational collisions. The effect of rotations decreases with increasing reduced electric field due to the decreasing fraction of low-energy electrons, together with an increase of importance of higher energy losses.

Collisional excitations from the vibrational ground state to the first vibrationally excited levels are included, see table 1. Due to the proximity of the thresholds of the stretching modes, they are not experimentally distinguishable and are described by a single CS. In literature, notations of 100 + 001 or 101 are found. Both vibrational CSs (∇), i.e. bending and stretching, are taken from Song *et al* [16], who in turn propose a combination of CS measured by Seng and Linder and Khakoo *et al* [39, 40].

The starting point for the excitation CSs for electronic states $\tilde{\text{A}}^1\text{B}_1$ and $\tilde{\text{a}}^3\text{B}_1$ (\otimes) are the CSs from measurements by Ralphs *et al* and Matsui *et al* [41, 42] as proposed by Song *et al* [16]. Both CSs are decreased by 10%, within the reported error margin, to obtain an agreement between calculated and measured electron swarm parameters. Additionally, multiple dissociation processes are included (\diamond). The production of hydroxyl radicals in the electronic ground state OH(X) and the excited state OH(A) is represented by CSs from Harb *et al* and Beenakker *et al* [43, 44]. Both are also recommended by Biagi [38]. The production of $\text{O}(^1\text{S}_0)$ is included by a CS from Kedzierski *et al*, increased by 30%, within the reported error margin, to improve the agreement with swarm parameters [45]. Finally, a CS is introduced to improve the agreement of the simulation with experiments for high reduced electric fields, denoted as H_2O^* on the left-hand side of figure 1 and plotted as \otimes like all electronic excitation processes. It is based on a CS by Möhlmann and de Heer for production of Balmer 3-2 emission, scaled up by a factor of 100. A similar treatment is adapted by Kawaguchi *et al* [14]. All modifications beyond a simple scaling by a constant factor can be comprehended from figure 2 that shows the original CSs, i.e. as taken from the [33, 38], in grey and the eventually proposed optimised CSs in the same colour as in figure 1.

The right-hand side of figure 1 displays the non-conservative processes. Three dissociative attachment CSs (\triangle) lead to the production of H^- , O^- and OH^- , respectively. The former two are taken from the Trinit database on LXCat [10, 31] while the latter is taken from Biagi's Magboltz v11.9 [38]. Apart from the production of H_2O^+ also the ionisation processes are dissociative and result in OH^+ , H^+ , O^+ , O^{2+} and H_2^+ , respectively. All ionisation CSs (\oplus)

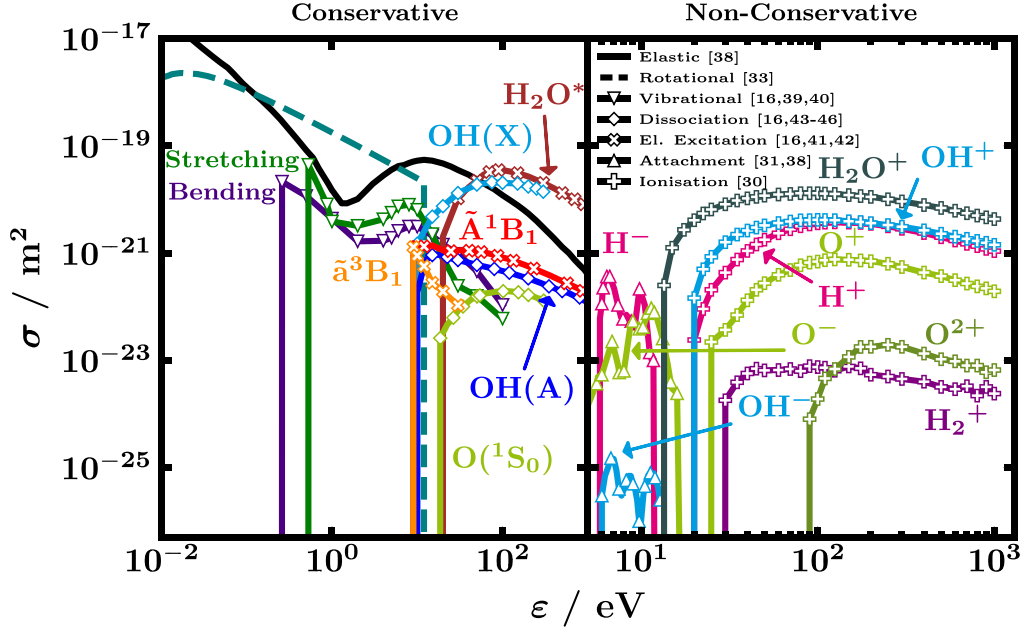


Figure 1. Proposed CSs σ , plotted against the electron energy ϵ , divided into conservative and non-conservative collisional processes without and with change in the number of electrons during the collision, respectively. The plotted rotational CS (dashed line) is the sum of all individual rotational CSs weighted by the populations of the lower rotational levels at 293 K. In the left-side panel, the elastic and rotational CS extend down to sub-meV range which is not shown for better visibility of the remaining conservative collision CSs. Original references of the CSs are given in the legend [16, 30, 31, 33, 38–46]. For a detailed record see table 2.

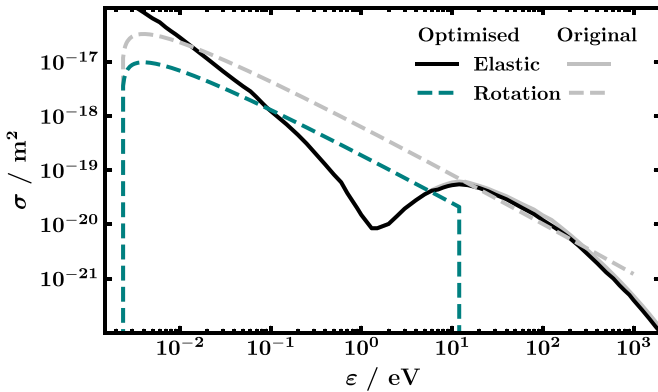


Figure 2. Comparison of optimised CSs σ , as proposed in figure 1, with the original unmodified CSs as taken from literature [33, 38] in grey plotted against the electron energy ϵ . For illustration, the rotational CS of transition $(JK'K'') = (110) \rightarrow (101)$ is arbitrarily chosen.

are taken from the Itikawa database on LXCat [10, 30]. The production of O^{2+} is treated like a single-ionisation event yielding one secondary electron in the electron growth model (temporal growth with equal energy sharing, see section 4). Since only a small fraction ($\sim 10^{-8}$) of the power deposited in total ionisation ends up in that particular ionisation channel, the error introduced by this simplified treatment is negligible.

All CSs in the set are summarised in table 2. A detailed list of the rotational transitions with thresholds and populations of the lower level can be found in the appendix in table 3.

4. Validation

The complete CS set presented in the previous section is validated by demonstrating that results obtained from a two-term Boltzmann solver are consistent with experimentally obtained electron swarm parameters from literature. Unless mentioned otherwise, all calculations in this paper are performed with the open-source code LoKI-B [8] to first obtain the general EEDF and then determine the swarm parameters from it. The required instructions, and setup as well as other input files are provided as supplementary material, see section D. In particular, the electron energy axis is divided in 2000 cells and 147 rotational CSs are incorporated. See appendices B and C for an assessment of the influence of these settings.

The electron swarm parameters are the electron drift velocity v_D [26, 53–61], the reduced mobility μN [53], the characteristic energy $\epsilon_{char} = D_T/\mu$ [62, 63], the reduced Townsend coefficient α/N [64, 65], the reduced attachment coefficient η/N [62, 64–67] and the reduced effective Townsend coefficient, defined as the difference of the latter two [54, 64, 65, 65]. Here, N is the total gas number density, μ the electron mobility, D_T the transverse diffusion coefficient, α the Townsend coefficient and η the attachment coefficient. When not given explicitly, the reduced mobility is calculated from $\mu N = v_D N/E$ with E being the electric field and E/N the reduced electric field, usually given in Townsend ($1Td = 10^{-21} \text{ V m}^2$). Swarm parameters for water are provided in a relatively narrow temperature range. The two extremes, namely the study by Bailey and Duncanson at 288 K and the one by Pack, Voshall, and Phelps at 400 K, do not appear to agree with the other studies [26, 53–55, 57–60] and, as a consequence, are discarded

Table 2. List of processes included in the proposed CS set.

#	Process	Product	Threshold (eV)	Reference
1	Elastic	H ₂ O		[38]
2	Rotational	H ₂ O(<i>X, v</i> = 000, <i>J</i> = 110)	0.00230	[33]
⋮		⋮		
148	Rotational	H ₂ O(<i>X, v</i> = 000, <i>J</i> = 551)	0.03663	[33]
149	Vibrational	H ₂ O(<i>X, v</i> = 010)	0.198	[16, 39, 40]
150	Vibrational	H ₂ O(<i>X, v</i> = 100 + 001)	0.453	[16, 39, 40]
151	Electronic Excitation	H ₂ O(\tilde{A}^1B_1)	7.49	[16, 41, 42]
152	Electronic Excitation	H ₂ O(\tilde{a}^3B_1)	7.14	[16, 41]
153	Dissociation	OH(<i>X</i>) + H(<i>X</i>)	6.6	[43]
154	Dissociation	OH(<i>A</i>) + H(<i>X</i>)	9.2	[44]
155	Dissociation	O(¹ S ₀) + 2H(<i>X</i>)	13.696	[16, 45]
155	Dissociation	H ₂ O*	18.0	[46]
156	Attachment	OH ⁻ (<i>X</i>) + H(<i>X</i>)	5.9	[38]
157	Attachment	O ⁻ (<i>X</i>) + H ₂ (<i>X</i>)	4.9	[31]
158	Attachment	H ⁻ (<i>X</i>) + OH(<i>X</i>)	5.7	[31]
159	Ionisation	H ₂ O ⁺	13.5	[30]
160	Ionisation	H ⁺ (<i>X</i>) + OH(<i>X</i>)	18.116	[30]
161	Ionisation	H ₂ (<i>X</i>) + O ⁺ (<i>X</i>)	19.0	[30]
162	Ionisation	H ₂ ⁺ (<i>X</i>) + O(<i>X</i>)	20.7	[30]
163	Ionisation	H ₂ (<i>X</i>) + O ²⁺ (<i>X</i>)	80.0	[30]

here [56, 61]. The remaining studies report measurements at room temperature, i.e. between 290 to 300 K, and the gas temperature in the calculations is set to 293 K accordingly. All swarm parameters extracted from literature will be made available in the IST-Lisbon database on LXCat together with the proposed CS set.

Figure 3 shows the comparison of the calculated swarm parameters (lines) with the experimentally determined ones (markers). Note that the reduced mobility and the reduced effective Townsend coefficient (both with *y*-axis labels on the right) are plotted linearly while all other parameters are presented in logarithmic scale. Whenever known, the uncertainty of the experimental swarm parameters is shown as error bars. From top to bottom of figure 3, v_D , μN , ε_{char} , η/N , $(\alpha - \eta)/N$ and α/N are shown. The bottom three panels display only the high reduced electric field range since non-conservative processes are only relevant there, due to the high thresholds of the corresponding CSs, compare figure 1. Temporal (solid green line) as well as spatial growth (dotted magenta line) of the electron number is tested [8]. The former is the default throughout this paper.

The most significant feature of the swarm parameters of water, namely a very steep increase between 30 to 80 Td, is best observed for the reduced mobility μN . As pointed out by Ness and Robson [15], this is due to the rapidly decreasing elastic CS, see figure 1. They show that, with a few simplifications, even a singularity would occur that is damped by vibrations, electronic excitations etc that dissipate the electron energy. In figure 4, the EEDFs of water, as calculated with LoKI-B, before (10 Td), during (60 Td) and after the strong increase (300 Td) are shown to illustrate the differences. Note that in any case the EEDF is strongly non-Maxwellian.

Even though the experimental swarm parameters are quite consistent, there is still some spread of data. For instance, the increase in η/N for decreasing E/N measured by Kuffel (○) in the last panel of figure 3 [66], that was originally interpreted as consequence of three-body processes, is probably rather caused by impurities [67]. The measurements of Prasad and Craggs (○) [65] for the reduced Townsend and attachment coefficient, deviate from other references. Especially, their η/N values could not be obtained with the available CSs and should be considered with care.

Additionally, the growth (model) of the electron number influences the outcome of simulations and measurements, as can be seen from the solid green and the dashed magenta line in figure 3. Usual configurations are pulsed Townsend (PT) and steady-state Townsend (SST) experiments, where the number of electrons grows, due to ionisation dominating over attachment, in time or in space, respectively [8, 27]. α/N and η/N are determined from SST experiments, while v_D (and thereby μ) and D_T are determined from PT experiments. Simulations should consider the proper growth model, depending on which experimental values they try to reproduce [17, 68]. The set is optimised assuming temporal growth in the calculations with LoKI-B. While this approach obviously reduces the amount of necessary simulation runs, it particularly facilitates the comparison with Monte Carlo codes that often (but not exclusively) follow the electrons in time rather than in space [27]. However, in the presented range of E/N the differences compared with the spatial growth model are negligible. The used growth model as well as other settings of the calculation can be found in the provided input file in the supplementary material.

The overall agreement of the calculations with the experimental swarm parameters is very good. In particular, the low

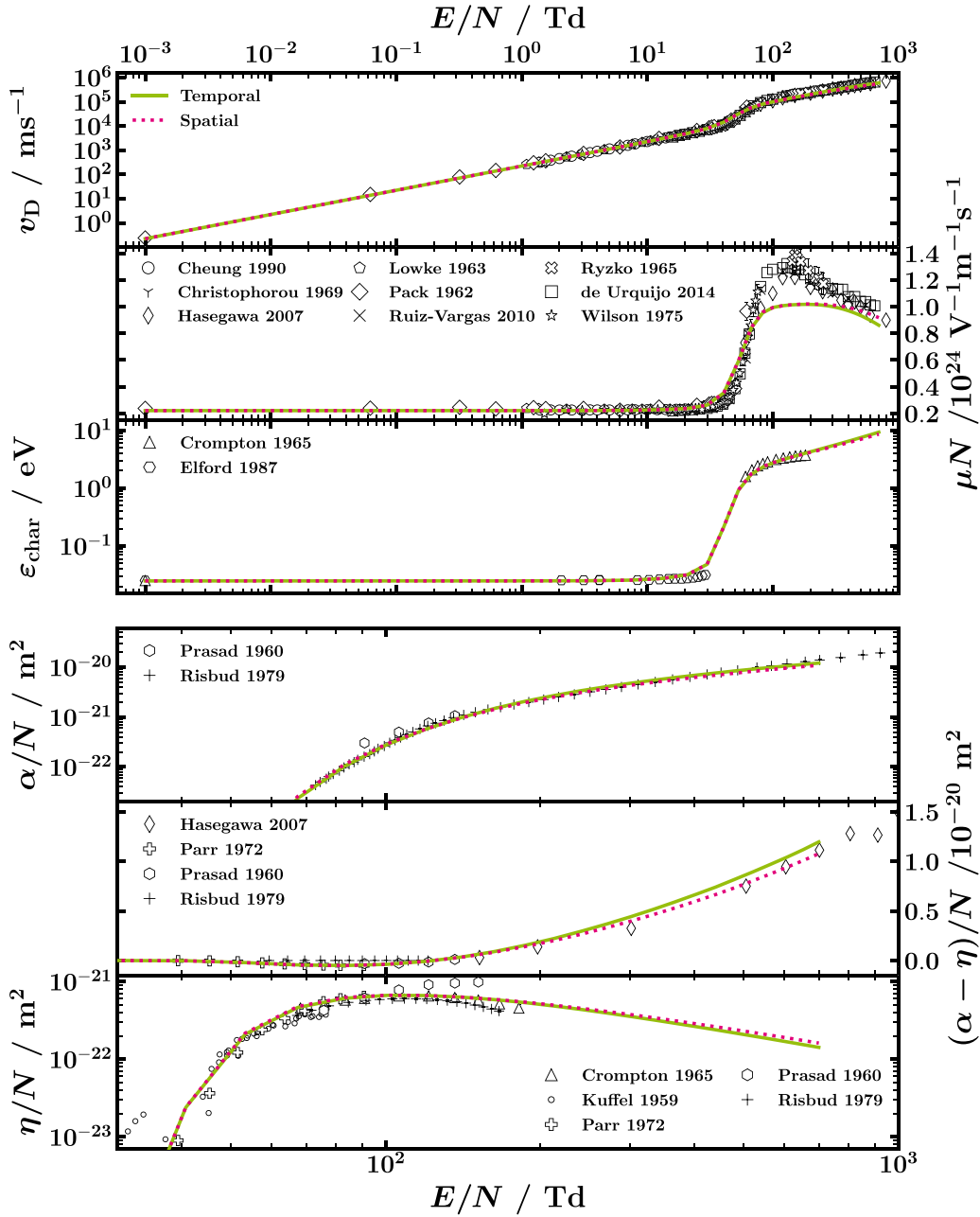


Figure 3. Comparison of experimental swarm parameters, when known with error bars, with those obtained from the LoKI-B simulation with the proposed CS set using either temporal (solid green line) or spatial growth (dotted magenta line) of the electron number [8]. Pay attention to (i) the linear y-axis scaling for panels with the y-label on the right-hand side, i.e. reduced mobility and reduced effective Townsend coefficient, and (ii) the smaller E/N range shown in the bottom three panels with respect to the top three. References to the experimental swarm parameters (markers) can be found in the text.

reduced electric field range, dominated by rotations, is represented excellently. The largest disagreement is found between 100 to 400 Td, especially for μN (note however, the linear scale of the figure). The maximum deviation from the experimental swarm parameters reaches up to 30%. While being most certainly not negligible, as the mobility influences the electron density when coupling the Boltzmann solver to a chemistry module, the agreement with parameters like α/N , that are expected to have an even larger effect on the chemistry, is excellent. We consider this a drawback of the presented isotropic set since the agreement with the anisotropic set is

improved as will be shown in a follow-up publication. However, the latter set is not usable in most Boltzmann solvers, which is why the former is a legitimate and useful compromise. The importance of our proposed set for the community is emphasised by comparing with results from other available sets as shown in figure 6 in the [appendix](#).

Wide-spread acceptance of the proposed CS set demands that its applicability is not limited to LoKI-B but in principle comprises any space-homogeneous isotropic code. Admittedly, a thorough check against any code is clearly out of the scope of this publication. Therefore, we only refer to

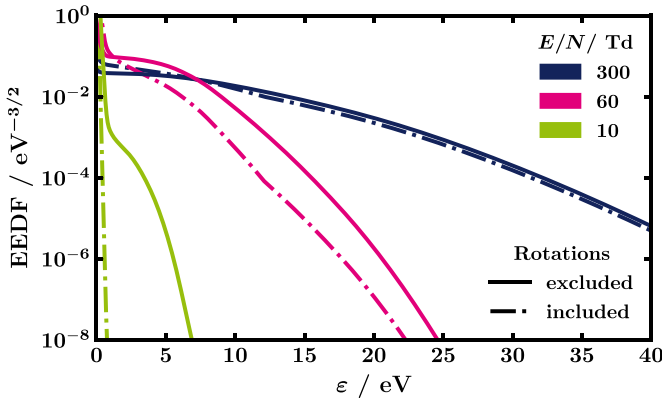


Figure 4. EEDFs of water calculated with LoKI-B [8] using the CS set proposed in figure 1 either including all 147 rotational transitions (dash-dotted lines) or completely excluding rotations (solid lines) for three different reduced electric fields E/N , namely 300, 60 and 10 Td in blue, magenta and green, respectively. Due to the increasing fraction of low-energy electrons, i.e. for which the rotational CSs are very large, with decreasing E/N the difference between the solid and the dash-dotted lines increases.

BOLSIG+ v11/19 since it is probably the most widely established two-term Boltzmann solver [9]. Its agreement with LoKI-B for atomic gases is proven [8]. For molecular gases like water, with inclusion of rotations and superelastic collisions, it is desirable to confirm. Eventually, this underpins the general validity of the CS set in space-homogeneous codes beyond LoKI-B.

The CSs are structured such that they can be parsed by LoKI-B and BOLSIG+ and describe the same physics. Primarily, rotational and vibrational states are populated correctly with respect to the gas temperature and superelastic collisions between them are included. When using the provided input file, LoKI-B automatically handles those aspects. Vibrational populations are manually entered in BOLSIG+, see table 1 at 293 K. Rotational populations are correctly calculated by BOLSIG+ by means of energy and statistical weight of each lower and upper rotational state as given with the CSs. Hence, any remaining differences between LoKI-B and BOLSIG+ are attributed to numeric reasons.

Figure 5 illustrates the differences between LoKI-B (solid green line) and BOLSIG+ (dashed blue line) based on the reduced attachment coefficient η/N plotted against the reduced electric field E/N when using all CSs from table 2, particularly all 147 rotational CSs, in both codes together with markers that represent experimental data [63–67]. A deviation up to 10% between the two codes is noticed. However, both obtained curves give reasonable agreement with the experimental data. Since all other swarm parameters show better agreement, we take the 10% as a maximum estimation of the numeric uncertainty. Despite BOLSIG+ not being open source, after some testing, we can attribute these discrepancies to the following reasons.

- (a) Extrapolation
BOLSIG+ by default extrapolates CSs beyond their upper energy limit according to $\log(\epsilon)/\epsilon$ while they are set to

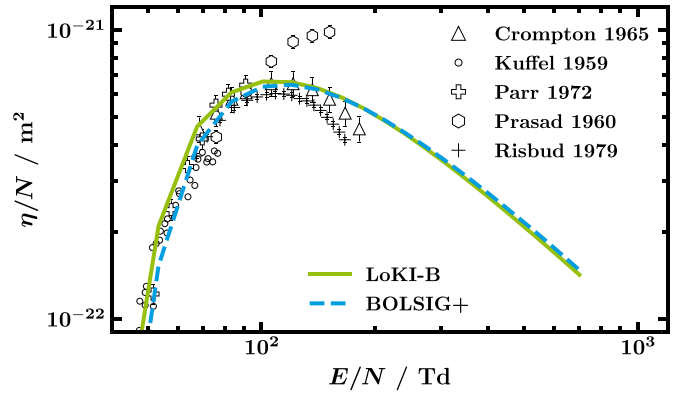


Figure 5. Comparison of the outcome of LoKI-B v2.1.0 and BOLSIG+ v11/19 for the same proposed isotropic set of CSs by means of the reduced attachment coefficient η/N against the reduced electric field E/N . Markers represent experimental swarm parameters.

zero by LoKI-B. For better comparison either the extrapolation is disabled in BOLSIG+ or the CSs are manually extrapolated following the $\log(\epsilon)/\epsilon$ energy dependence before using them in LoKI-B. The latter option is tested and reveals only a minor influence of the extrapolation.

- (b) Population normalisation
BOLSIG+ applies the normalisation condition to each superelastic excitation, particularly vibrational, collisional process separately by means of bi-Maxwellian Boltzmann factors while LoKI-B normalises over the full vibrational manifold. The vibrational populations as in table 1 are entered manually in BOLSIG+ to mitigate the influence of the population normalisation. Tests prove the influence of the normalisation to be negligible at 293 K though.
- (c) Effective CS
Strictly speaking, we do not know how BOLSIG+ calculates the effective CS. We expect it to rely on the sum of elastic momentum transfer and inelastic CSs weighted by the fractional populations which connects this point to point (ii) as BOLSIG+ treats rovibrational states as individual species. Thus, we must consider this a major difference between the codes that is not further quantifiable.
- (d) Energy axis
The number of cells used to probe the energy axis that is scaled automatically to the maximum electron energy for both codes might not resolve the very low-energy thresholds of the rotational CSs. Also, the way the axis is scaled might be different. To minimise this component, the same number of cells (2000) is used in both codes to obtain figure 5. In LoKI-B the EEDF is set to span ten to fifteen decade-falls. As shown in figure 7 in the appendix, the number of cells used in LoKI-B significantly influences η/N (and α/N) as well, which is why we suspect the energy discretisation to be the dominating aspect in the difference between LoKI-B and BOLSIG+.

The points above only address differences between the codes. General advantages over one another, e.g. the more advanced physical models like magnetised plasma in

BOLSIG+ [9] or the full consideration of the internal state of an atom or molecule in LoKI-B [8], are acknowledged. Nonetheless, they are of secondary importance here as the point to be made is the universal applicability of our CS set in space-homogeneous codes with different foci. We refer to the manuals of both codes for more details.

5. Conclusion

Even though water is a frequently encountered molecule in many innovative plasma applications, the community still lacks a commonly accessible, complete and consistent electron collision CS set with H₂O which is required for the determination of the EEDF. While there is agreement on the significant influence of molecular rotations of water on the EEDF, particularly in the low-energy range, there is less consensus on how to include them. Here, we propose a CS set that addresses that predicament by optimising rotational CSs based on the Born approximation for dipole transitions by means of the electron swarm technique. Of the 163 CSs in the set 147 are rotational. The remaining CSs describe elastic, vibrational, electronic excitation, dissociation, attachment and ionisation collisions. The comparison of results of calculations with the two-term Boltzmann solver LoKI-B with experimental electron swarm parameters obtains good agreement, hence validating the proposed set. It allows simulations, performed with a common two-term solver, to consider water within reasonable calculation time and accuracy. Thereby, the set promotes the development of more sophisticated plasma chemistry models and consequently facilitates the understanding and optimisation of experiments and applications. The set will be made available to the community in the IST-Database on LXCat [32]. A future study will investigate the importance of anisotropy in scattering events.

Data availability statement

All data that support the findings of this study are included within the article (and any supplementary files).

Acknowledgments

The authors acknowledge the comments of Luís Lemos Alves, particularly regarding the use of BOLSIG+. This work was partially supported by the European Union's Horizon 2020 research and innovation programme under Grant Agreement MSCA ITN 813393, by Portuguese FCT-Fundação para a Ciência e a Tecnologia, under Projects UIDB/50010/2020, UIDP/50010/2020 and PTDC/FIS-PLA/1616/2021 (PARA-DiSE), Grant PD/BD/150414/2019 (PD-F APPLAuSE) and EXPL/FIS-PLA/0076/2021. L V acknowledges fundings from Deutsche Forschungsgemeinschaft (DFG, German Research Foundation)—Project-ID 434434223 - SFB 1461.

Appendix A. Comparison with other databases

Even though there are published compilations of CSs that are certainly valuable options to pick from, these compilations are often not complete and consistent sets of CSs. To further motivate the need for our work presented here, in figure 6 the electron swarm parameters calculated from LoKI-B using our recommended set (solid green line), the CSs from Song *et al* [16] (dashed orange line) and the Itikawa database on LXCat [30] (dash-dotted blue line) are plotted against E/N together with experimental swarm parameters (markers). The former CS set is an update of the latter which is in turn based on [13]. The solid green line is the same as in figure 3.

Song *et al* and the Itikawa database are chosen since they present relatively recent extensive compilations of H₂O CSs both including rotations. Song *et al* provide in their supplementary material state-to-state rotational CSs ($JK'K''$) that only need to be transferred to LoKI-B/BOLSIG+-readable format. All other CSs are taken *as is* from the tables in the publication. On the other hand, the Itikawa database only includes lumped rotational CSs ($J = 0 \rightarrow 0, 1, 2, 3$). As effective rotational energy levels the thresholds of the four transitions are used, as effective statistical weight $2J + 1$ is assumed. Finally, for both sets the given partial ionisation CSs are used, i.e. the total ionisation CS is removed.

It is immediately visible from figure 6 that in contrast to our recommended CS set neither Song *et al* nor Itikawa give a satisfying agreement with experimental swarm parameters. From the drift velocity in the first panel it appears that the Itikawa set gives reasonable agreement with experiments. However, a look at the second panel showing the reduced mobility calculated from $v_D N/E$, i.e. principally the same data as in the first panel but in linear scale, reveals a strong disagreement also for Itikawa. For the reduced Townsend and attachment coefficient in the fourth and sixth panel a better agreement with experiments and the proposed CS set is observed for E/N higher than 150 Td. Since the ionisation CSs in our set are taken from the Itikawa database [30], see table 2, and CSs from Song *et al* [16] exhibit only slight changes compared to Itikawa and Mason's CSs, this behaviour is expected. For the reduced effective Townsend coefficient in the fifth panel, i.e. the difference between α/N and η/N , the opposite trend is observed with a better agreement of Itikawa and Song for low E/N . We attribute this to two deviations cancelling each other, see the strong divergence from experimental values for α/N and η/N below 150 Td. Note also the linear scale in that panel. Overall, the disagreement between experiments and calculations using CSs from Itikawa and Song is not surprising, as the purpose of their studies is different from ours. By means of a vast comparison of literature, they are able to give excellent individual CSs of water. We on the other hand focused on the entire set from the very beginning and optimised it accordingly by the electron swarm method to obtain the good agreement shown in figure 6, despite applied simplifications like rotational CSs calculated from the Born approximation.

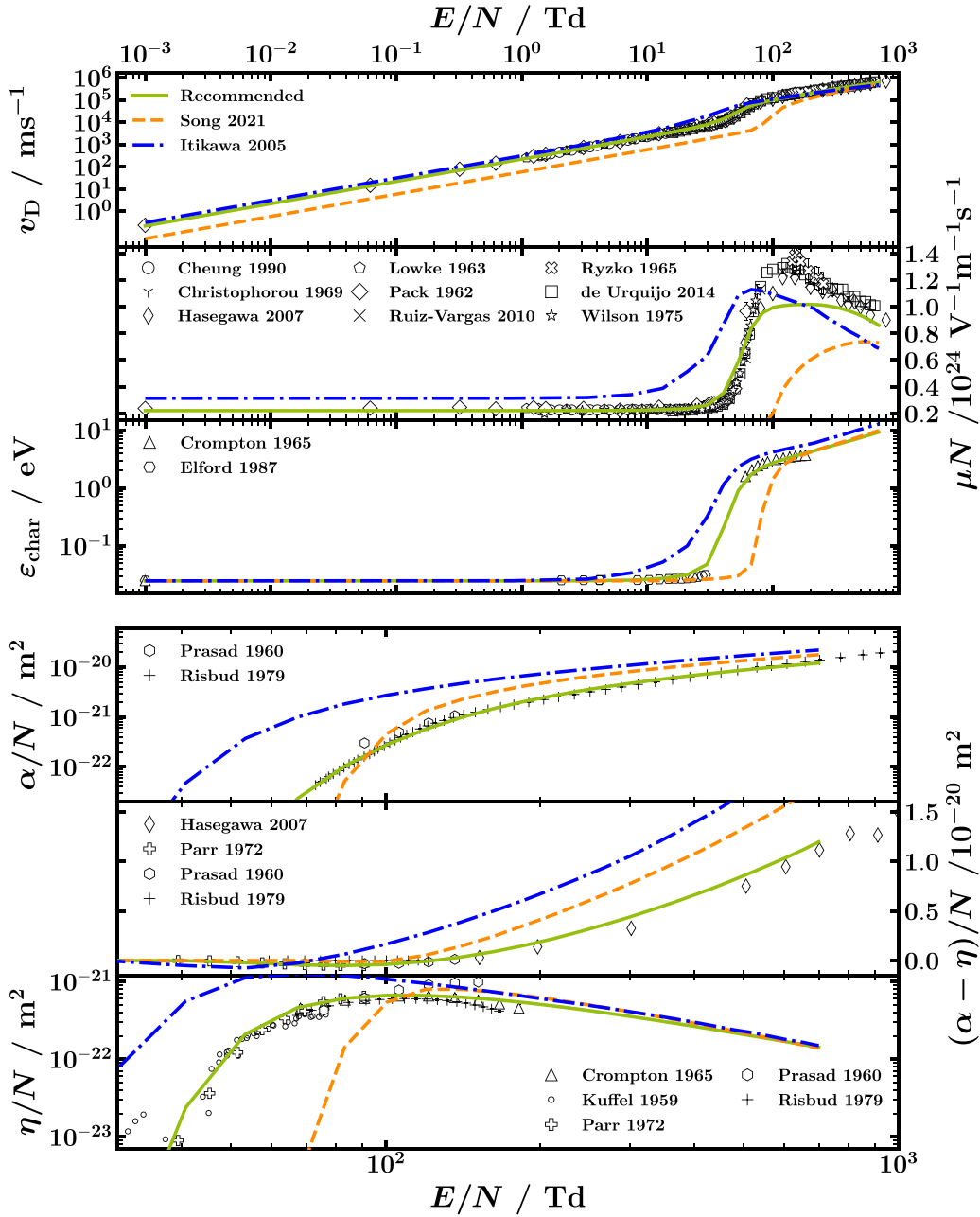


Figure 6. Comparison of experimental swarm parameters, when known with error bars, with those obtained from the LoKI-B simulation with the recommended CS set (solid green line), the one from Song *et al* [16] (dashed orange line) and the one from the Itikawa database on LXCat [30], originally based on Itikawa and Mason [13] (dash-dotted blue line). Pay attention to (i) the linear y-axis scaling for panels with the y-label on the right-hand side, i.e. reduced mobility and reduced effective Townsend coefficient, and (ii) the smaller E/N range shown in the bottom three panels with respect to the top three. References to the experimental swarm parameters (markers) can be found in the text.

Appendix B. Influence of the energy discretisation

The difficulties mentioned in the main text regarding the choice of the number of cells that the electron energy axis is divided in, deserve some further discussion. Because the thresholds of the rotational transitions are very small, see for instance table 3, i.e. reaching down to the sub-meV range, they cannot be resolved by the minimum energy increment of commonly advised cell numbers. For instance, in the latest version of LoKI-B the default cell numbers are 1000 for Ar, CO, CO₂,

and He and 2000 for N₂ and O₂. Noticeable differences are observed when integrating over the EEDF to obtain the swarm parameters depending on the used number of cells.

This is illustrated in figure 7, where the deviation of the calculation results and the required calculation time are plotted against the used cell number. Apart from the cell number the settings are the same as in figure 5 which means the Boltzmann equation is solved for thirty values of E/N between 0.01 and 700 Td. Assuming the results get more and more accurate with increasing cell number, i.e. the results with 9000 cells are the

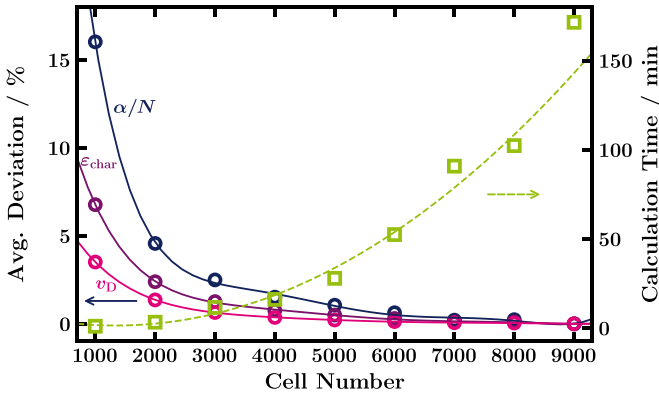


Figure 7. Percentage deviation of swarm parameters with respect to the results for 9000 cells (circles, left) and calculation time (squares, right) plotted against the used number of cells to discretise the energy axis in the calculation with LoKI-B. Lines are polynomial fits to the data to serve as guides to the eye.

best of the recorded sample, all other results are related to the latter. The deviation of the results per swarm parameter is represented by means of the average absolute percentage difference with respect to the outcome when using 9000 cells and hence the average deviation of 9000 cells is 0%. The lines in figure 7 are polynomial fits meant as guides to the eye. The dashed green line confirms the expected quadratic increase of calculation time with cell number (within performance variations of the used PC).

Higher resolution by an increased number of cells comes with the cost of increased calculation time. For instance, for LoKI-B we find the results to be independent of the number of cells, when at least 8000 cells are included in the calculations. However, the calculation time is then unfeasible for coupling to chemical kinetics. Therefore, we recommend 2000 cells to be used for the isotropic set. Reduced Townsend and attachment coefficient show the largest deviation (as they are more or less identical only the deviation for α/N is plotted) that is still less than 5% with respect to 9000 cells for the recommended number of cells, i.e. 2000.

Appendix C. Rotational transitions

For completeness, all considered rotational transitions are given in table 3 ordered by the magnitude of the rotational CS weighted by the population of the lower state. Even though the large number of rotational transitions ensures the proper behaviour with changing temperature, from a fluid modelling point of view it is less desirable. To evaluate the compromise of reducing the number of transitions considered see figure 8. It turns out that the 80 largest rotational CS at 293 K still give almost the same swarm parameters. Afterwards large deviations are observed. The calculation time is mostly unaffected by the number of CS. We recommend to always use the total number of 147 rotational CS.

Table 3. Considered rotational transitions of water $J \rightarrow J'$ with respective threshold taken from Tennyson *et al* and population of lower state assuming a Boltzmann distribution at 293 K [37]. Numbering as in table 2.

#	J	J'	Threshold (eV)	Population
2	101	110	0.00230	0.01496
3	303	312	0.00454	0.02004
4	312	321	0.00481	0.01674
5	101	212	0.00691	0.01496
6	212	303	0.00710	0.01896
7	202	211	0.00311	0.00662
8	303	414	0.01092	0.02004
9	110	221	0.01147	0.01365
10	414	505	0.01246	0.01672
11	514	523	0.00583	0.00867
12	212	221	0.00687	0.01896
13	000	111	0.00460	0.00187
14	505	616	0.01512	0.01247
15	523	616	0.00009	0.00688
16	221	330	0.01866	0.01444
17	413	422	0.00499	0.00435
18	202	313	0.00895	0.00662
19	414	423	0.00936	0.01672
20	312	423	0.01575	0.01674
21	211	220	0.00508	0.00585
22	111	202	0.00409	0.00467
23	523	532	0.00773	0.00688
24	313	404	0.00989	0.00650
25	321	330	0.00908	0.01384
26	505	514	0.00919	0.01247
27	423	432	0.01019	0.01154
28	321	432	0.02112	0.01384
29	212	321	0.01645	0.01896
30	404	413	0.00663	0.00565
31	404	515	0.01297	0.00565
32	330	441	0.02513	0.00966
33	221	312	0.00477	0.01444
34	423	514	0.01229	0.01154
35	111	220	0.01228	0.00467
36	321	414	0.00157	0.01384
37	313	322	0.00794	0.00650
38	211	322	0.01378	0.00585
39	514	625	0.01903	0.00867
40	220	313	0.00076	0.00479
41	515	606	0.01489	0.00413
42	220	331	0.01848	0.00479
43	422	431	0.00844	0.00357
44	432	541	0.02825	0.00771
45	330	423	0.00185	0.00966
46	625	634	0.01191	0.00482
47	423	532	0.02585	0.01154
48	616	625	0.01310	0.00810
49	532	541	0.01259	0.00507
50	615	624	0.00742	0.00169
51	322	331	0.00979	0.00475
52	441	550	0.03149	0.00459
53	432	441	0.01309	0.00771

(Continued.)

Table 3. (Continued.)

#	J	J'	Threshold (eV)	Population
54	413	524	0.01745	0.00435
55	322	431	0.02201	0.00475
56	322	413	0.00858	0.00475
57	624	633	0.00729	0.00126
58	331	440	0.02516	0.00322
59	523	634	0.02511	0.00688
60	515	524	0.01111	0.00413
61	524	533	0.01088	0.00266
62	634	643	0.01336	0.00301
63	532	643	0.03074	0.00507
64	432	523	0.00794	0.00771
65	524	615	0.01571	0.00266
66	422	533	0.02333	0.00357
67	541	652	0.03450	0.00308
68	431	542	0.02806	0.00255
69	606	615	0.01193	0.00271
70	532	625	0.00547	0.00507
71	422	515	0.00134	0.00357
72	313	422	0.02151	0.00650
73	414	523	0.02749	0.01672
74	533	542	0.01316	0.00173
75	431	440	0.01293	0.00255
76	440	551	0.03149	0.00153
77	441	532	0.00257	0.00459
78	550	661	0.03757	0.00161
79	331	422	0.00379	0.00322
80	541	550	0.01633	0.00308
81	633	642	0.01193	0.00094
82	431	524	0.00401	0.00255
83	643	652	0.01635	0.00177
84	541	634	0.00479	0.00308
85	533	642	0.03147	0.00173
86	542	651	0.03454	0.00103
87	524	633	0.03042	0.00266
88	533	624	0.01225	0.00173
89	440	533	0.00196	0.00153
90	550	643	0.00182	0.00161
91	551	660	0.03757	0.00054
92	542	551	0.01636	0.00103
93	642	651	0.01623	0.00059
94	303	432	0.03047	0.02004
95	542	633	0.00638	0.00103
96	652	661	0.01940	0.00093
97	505	634	0.04013	0.01247
98	505	532	0.02275	0.01247
99	515	624	0.03424	0.00413
100	303	330	0.01843	0.02004

(Continued.)

Table 3. (Continued.)

#	J	J'	Threshold (eV)	Population
101	551	642	0.00195	0.00054
102	505	432	0.00709	0.01247
103	404	533	0.03496	0.00565
104	404	431	0.02006	0.00565
105	651	660	0.01940	0.00031
106	514	643	0.04430	0.00867
107	514	541	0.02615	0.00867
108	202	331	0.02668	0.00662
109	606	533	0.00710	0.00271
110	615	642	0.02664	0.00169
111	606	633	0.02664	0.00271
112	404	331	0.00783	0.00565
113	312	441	0.03903	0.01674
114	413	542	0.04149	0.00435
115	414	541	0.04780	0.01672
116	615	542	0.00833	0.00169
117	514	441	0.01099	0.00867
118	413	440	0.02637	0.00435
119	523	652	0.05482	0.00688
120	616	643	0.03837	0.00810
121	414	441	0.03264	0.01672
122	515	642	0.05346	0.00413
123	625	652	0.04162	0.00482
124	515	542	0.03515	0.00413
125	423	550	0.05477	0.01154
126	313	440	0.04288	0.00650
127	523	550	0.03665	0.00688
128	624	651	0.03545	0.00126
129	524	651	0.05858	0.00266
130	616	541	0.02022	0.00810
131	422	551	0.05286	0.00357
132	532	661	0.06649	0.00507
133	524	551	0.04041	0.00266
134	634	661	0.04911	0.00301
135	515	440	0.02003	0.00413
136	505	652	0.06984	0.01247
137	625	550	0.02346	0.00482
138	533	660	0.06709	0.00173
139	624	551	0.01727	0.00126
140	633	660	0.04755	0.00094
141	404	551	0.06448	0.00565
142	606	651	0.05480	0.00271
143	616	661	0.07413	0.00810
144	615	660	0.06227	0.00169
145	515	660	0.08908	0.00413
146	505	550	0.05167	0.01247
147	514	661	0.08005	0.00867
148	606	551	0.03663	0.00271

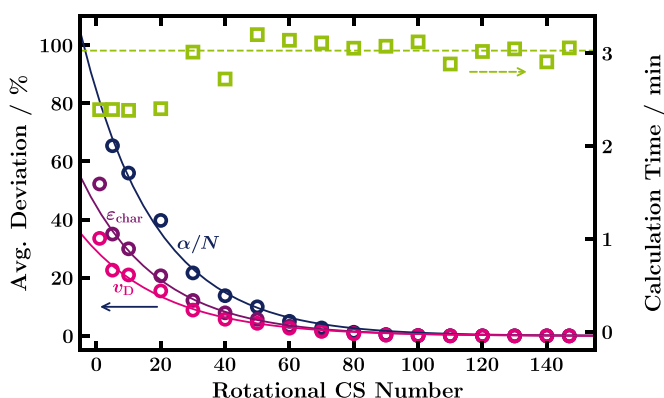


Figure 8. Percentage deviation of swarm parameters with respect to the results for 147 included rotational CSs (circles, left) and calculation time (squares, right) plotted against the used number of largest rotational CSs in the calculation with LoKI-B. Lines are fits to the data to serve as guides to the eye. 2000 cells are used.

Appendix D. Provided files and instructions

The following files are provided with this manuscript:

- `rotationalDegeneracy_H2O.m`

A Matlab function to calculate the statistical weight of rotational levels of water under consideration of the differences between ortho- and para-water. The function is easily coupled to the open-source code LoKI-B where it is used in the input file (provided as well) by means of

```

statisticalWeight:
- H2O(X, v = 000, J = *)
  = rotationalDegeneracy_H2O
...

```

but can also serve as stand-alone function.

- `rotEnergy_Tennyson.txt`

A Text file containing a two-column table with the rotational state in the first and its corresponding energy in the second column. It is needed for the calculation of the rotational populations in LoKI-B by the line

```

energy:
- Water/H20_rotEnergy_Tennyson.txt
...

```

in the input file (assuming all the energy files to be contained in the input subfolder Water).

- `vibEnergy_Itikawa.txt`

Another Text file that gives the same data for the vibrational levels

```

energy:
- Water/H20_vibEnergy_Itikawa.txt
...

```

- `H2O_swarm_setup.in`

The input file used to control the calculations by LoKI-B. We refer to [8] for details on the usage. In the optimisation 2000 cells, equal energy sharing between primary and secondary electrons and temporal electron number growth are used.

ORCID iDs

Maik Budde <https://orcid.org/0000-0002-9084-4471>
 Tiago Cunha Dias <https://orcid.org/0000-0002-2179-1345>
 Luca Vialetto <https://orcid.org/0000-0003-3802-8001>
 Nuno Pinhão <https://orcid.org/0000-0002-4185-2619>
 Vasco Guerra <https://orcid.org/0000-0002-6878-6850>
 Tiago Silva <https://orcid.org/0000-0001-9046-958X>

References

- [1] Grosse K, Falke M and von Keudell A 2021 *J. Appl. Phys.* **129** 213302
- [2] Pawłat J, Terebun P, Kwiatkowski M and Wolny-Koładka K 2021 *Water* **13** 194
- [3] Shimizu T 2020 *Jpn. J. Appl. Phys.* **59** 120501
- [4] Winter J, Wende K, Masur K, Iseni S, Dünnbier M, Hammer M U, Tresp H, Weltmann K D and Reuter S 2013 *J. Phys. D: Appl. Phys.* **46** 295401
- [5] Chang Y, Mendrea B, Sterniak J and Bohac S V 2016 *J. Eng. Gas Turbines Power* **139** 051501
- [6] Kogelheide F, Voigt F, Hillebrand B, Moeller R, Fuchs F, Gibson A R, Awakowicz P, Stapelmann K and Fiebrandt M 2020 *J. Phys. D: Appl. Phys.* **53** 295201
- [7] Damen M A, Martini L M and Engeln R 2020 *Plasma Sources Sci. Technol.* **29** 095017
- [8] Tejero-del-Caz A, Guerra V, Gonçalves D, Silva M L D, Marques L, Pinhão N, Pintassilgo C D and Alves L L 2019 *Plasma Sources Sci. Technol.* **28** 043001
- [9] Hagelaar G J M and Pitchford L C 2005 *Plasma Sources Sci. Technol.* **14** 722–33
- [10] Carbone E, Graef W, Hagelaar G, Boer D, Hopkins M M, Stephens J C, Yee B T, Pancheshnyi S, van Dijk J and Pitchford L 2021 *Atoms* **9** 16
- [11] Anzai K et al 2012 *Eur. Phys. J. D* **66** 36
- [12] Hayashi M 1989 Electron collision cross-sections for atoms and molecules determined from beam and swarm data *Technical Report IAEA-TECDOC-506* (International Atomic Energy Agency (IAEA)) (available at: http://inis.iaea.org/search/search.aspx?orig_q=RN:20064036)
- [13] Itikawa Y and Mason N 2005 *J. Phys. Chem. Ref. Data* **34** 1–22
- [14] Kawaguchi S, Takahashi K, Satoh K and Itoh H 2016 *Jpn. J. Appl. Phys.* **55** 07LD03
- [15] Ness K F and Robson R E 1988 *Phys. Rev. A* **38** 1446–56
- [16] Song M Y, Cho H, Karwasz G P, Kokoouline V, Nakamura Y, Tennyson J, Faure A, Mason N J and Itikawa Y 2021 *J. Phys. Chem. Ref. Data* **50** 023103
- [17] Yousfi M and Benabdessadok M 1997 *J. Appl. Phys.* **80** 6619–30
- [18] Verheyen C, Silva T, Guerra V and Bogaerts A 2020 *Plasma Sources Sci. Technol.* **29** 095009
- [19] Faure A, Gorfinkiel J D and Tennyson J 2004 *Mon. Not. R. Astron. Soc.* **347** 323–33
- [20] Faure A, Gorfinkiel J D and Tennyson J 2004 *J. Phys. B: At. Mol. Opt. Phys.* **37** 801–7
- [21] Nishimura T and Itikawa Y 1995 *J. Phys. B: At. Mol. Opt. Phys.* **28** 1995–2005
- [22] Nishimura T and Gianturco F A 2004 *Eur. Phys. J.* **65** 179–85
- [23] Rescigno T and Lengsfeld B 1992 *Z. Phys. D: At., Mol. Clusters* **24** 117–24
- [24] van Harrevelt R and van Hemert M C 2000 *J. Chem. Phys.* **112** 5777–86
- [25] Winter N W, Goddard III W A and Bobrowicz F W 1975 *J. Chem. Phys.* **62** 4325–31

- [26] de Urquijo J, Basurto E, Juárez A M, Ness K F, Robson R E, Brunger M J and White R D 2014 *J. Chem. Phys.* **141** 014308
- [27] Alves L L, Bogaerts A, Guerra V and Turner M M 2018 *Plasma Sources Sci. Technol.* **27** 023002
- [28] Morgan database (available at: www.lxcat.net/Morgan) (Accessed 9 December 2021)
- [29] Phelps database (available at: www.lxcat.net/Phelps) (Accessed 9 December 2021)
- [30] Itikawa database (available at: www.lxcat.net/Itikawa) (Accessed 9 December 2021)
- [31] Trinitite database (available at: www.lxcat.net/Trinitite) (Accessed 9 December 2021)
- [32] Alves L L 2014 *J. Phys.: Conf. Ser.* **565** 012007
- [33] Itikawa Y 1972 *J. Phys. Soc. Jpn.* **32** 217–26
- [34] Ogloblina P, Tejero-del-Caz A, Guerra V and Alves L L 2020 *Plasma Sources Sci. Technol.* **29** 015002
- [35] Jung K, Antoni T, Muller R, Kochem K H and Ehrhardt H 1982 *J. Phys. B: At. Mol. Phys.* **15** 3535–55
- [36] Šimečková M, Jacquemart D, Rothman L S, Gamache R R and Goldman A 2006 *J. Quant. Spectrosc. Radiat. Transfer* **98** 130–55
- [37] Tennyson J, Zobov N F, Williamson R, Polyansky O L and Bernath P F 2001 *J. Phys. Chem. Ref. Data* **30** 735–831
- [38] Magboltz 11.9 (available at: <https://magboltz.web.cern.ch/magboltz/>) (Accessed 10 March 2022)
- [39] Seng G and Linder F 1976 *J. Phys. B: Atom. Mol. Phys.* **9** 2539–51
- [40] Khakoo M A, Winstead C and McKoy V 2009 *Phys. Rev. A* **79** 052711
- [41] Ralphs K, Serna G, Hargreaves L R, Khakoo M A, Winstead C and McKoy V 2013 *J. Phys. B: At. Mol. Opt. Phys.* **46** 125201
- [42] Matsui M, Hoshino M, Kato H, da Silva F F, Limão-Vieira P and Tanaka H 2016 *Eur. Phys. J. D* **70** 77
- [43] Harb T, Kedzierski W and McConkey J W 2001 *J. Chem. Phys.* **115** 5507–12
- [44] Beenakker C I M, de Heer F J, Krop H B and Möhlmann G R 1974 *Chem. Phys.* **6** 445–54
- [45] Kedzierski W, Derbyshire J, Malone C and McConkey J W 1998 *J. Phys. B: At. Mol. Opt. Phys.* **31** 5361–8
- [46] Möhlmann G R and de Heer F J 1979 *Chem. Phys.* **40** 157–62
- [47] Sullivan J P, Makochekanwa C, Jones A, Caradonna P, Slaughter D S, Machacek J, McEachran R P, Mueller D W and Buckman S J 2011 *J. Phys. B: At. Mol. Opt. Phys.* **44** 035201
- [48] Vialetto L, Moussa A B, van Dijk J, Longo S, Diomede P, Guerra V and Alves L L 2021 *Plasma Sources Sci. Technol.* **30** 075001
- [49] Takayanagi K 1966 *J. Phys. Soc. Jpn.* **21** 507–14
- [50] Shimamura I and Takayanagi K 2013 *Electron-Molecule Collisions* (Berlin: Springer)
- [51] King G W, Hainer R M and Cross P C 1947 *Phys. Rev.* **71** 433–43
- [52] Song M Y, Yoon J S, Cho H, Karwasz G P, Kokooouline V, Nakamura Y and Tennyson J 2019 *J. Phys. Chem. Ref. Data* **48** 043104
- [53] Cheung B and Elford M T 1990 *Aust. J. Phys.* **43** 755–63
- [54] Hasegawa H, Date H and Shimozuma M 2007 *J. Phys. D: Appl. Phys.* **40** 2495–8
- [55] Lowke J J and Rees J A 1963 *Aust. J. Phys.* **16** 447–53
- [56] Pack J L, Voshall R E and Phelps A V 1962 *Phys. Rev.* **127** 2084–9
- [57] Ruíz-Vargas G, Yousfi M and de Urquijo J 2010 *J. Phys. D: Appl. Phys.* **43** 455201
- [58] Ryzko H 1965 *Proc. Phys. Soc.* **85** 1283–95
- [59] Wilson J F, Davis F J, Nelson D R, Compton R N and Crawford O H 1975 *J. Chem. Phys.* **62** 4204–12
- [60] Christophorou L G and Christodoulides A A 1969 *J. Phys. B: Atom. Mol. Phys.* **2** 71–85
- [61] Bailey V A and Duncanson W E 1930 *London, Edinburgh Dublin Phil. Mag. J. Sci.* **10** 145–60
- [62] Elford M T 1987 The radio DT/ μ for electrons in water vapour at 294 K and low E/n values *Proc. 18th Int. Conf. on the Phenomena in Ionized Gases* (Swansea: Hilger) p 130
- [63] Crompton R W, Rees J A and Jory R L 1965 *Aust. J. Phys.* **18** 541
- [64] Risbud A V and Naidu M S 1979 *J. Phys. Colloques* **40** C7–C7–78
- [65] Prasad A N and Craggs J D 1960 *Proc. Phys. Soc.* **76** 223–32
- [66] Kuffel E 1959 *Proc. Phys. Soc.* **74** 297–308
- [67] Parr J E and Moruzzi J L 1972 *J. Phys. D: Appl. Phys.* **5** 514–24
- [68] Pitchford L C et al 2013 *J. Phys. D: Appl. Phys.* **46** 334001